DOI: 10.1021/ic1011633

Inorganic Chemistry
Article

Novel Three-Dimensional Metal-Azide Network Induced by a Bipyridine-Based Zwitterionic Monocarboxylate Ligand: Structures and Magnetism

Yu Ma,[†] Xiu-Bing Li,[†] Xiu-Chun Yi,[†] Qin-Xiang Jia,[†] En-Qing Gao,*[,†] and Cai-Ming Liu[‡]

[†]*Shanghai Key Laboratory of Green Chemistry and Chemical Processes, Department of Chemistry, East China Normal University, Shanghai 200062, China, and* [‡]*Institute of Chemistry, Chinese Academy of Sciences, Beijing 100190, China*

Received June 9, 2010

The 4,4′-bipyridine-based zwitterionic monocarboxylate ligand, 4,4′-dipyridinio-1-acetate (L), is used as coligand to construct novel magnetic coordination polymers with mixed azide and carboxylate bridges. Two compounds, $[Co_2(L)_2(N_3)_4(H_2O)]\cdot 4H_2O$ (**1**) and $[Mn_6(L)_4(N_3)_{12}(H_2O)]\cdot 5H_2O$ (**2**), have been structurally and magnetically characterized. Compound **1** consists of one-dimensional (1D) coordination chains in which the unprecedented binuclear motifs with mixed (μ-EO-N_3)(μ-COO)$_2$ (EO = end-on) triple bridges are cross-linked by the 4,4′-dipyridinium-*N*-methylene spacers. In compound **2**, the azide anions link the metal ions into a very complicated three-dimensional (3D) network with unprecedented topology, and the zwitterionic coligand is embedded in and serves as additional supports for the 3D network. Magnetic studies reveal that the mixed (μ-EO-N_3)(μ-COO)$_2$ triple bridges transmit ferromagnetic coupling in the Co(II) compound, and the overall antiferromagnetic interactions exist in the Mn(II) compound.

Introduction

Research on molecular magnetic materials has been of great interest for decades, with focus on understanding fundamental magnetic phenomena and designing new magnetic materials with potential applications.[1−3] Connecting paramagnetic centers by short bridges, in combination with incorporating different organic coligands to adjust the bridging structure and dimensionality, is a general strategy to design such materials.[4,5] Azide is among the most extensively studied short bridges, for its versatility in building extended networks and the diversity of the compounds in magnetic behavior.[5] Recently, particular attention has been focused on magnetic systems with three-dimensional (3D) metal-azide networks.[6−10] However, the 3D metal-azide networks without additional supporting bridges are rare, including a few neutral networks with the terminal organic ligands,[6,7] and a

*To whom correspondence should be addressed. E-mail: eqgao@chem.ecnu.edu.cn.

(1) (a) *Magnetism: Molecules to Materials*; Miller, J. S., Drilon, M., Eds.; Wiley-VCH: Weinheim, Germany, 2002−2005; Vol. *I*−*V*. (b) Kahn, O. *Molecular Magnetism*; VCH: New York, 1993. (c) Gatteschi, D.; Kahn, O.; Miller, J.-S.; Palacio, F. *Magnetic Molecular Materials*; Kluwer Academic: Dordrecht, The Netherlands, 1991.

(2) (a) Special issue on Magnetism - Molecular, Supramolecular Perspectives *Coord. Chem. Rev.* **2005**, *321*, 249. (b) *Molecular Magnetism: from Molecular Assemblies to Devices*; Coronado, E., Delhaes, P., Gatteschi, D., Miller, J.-S., Eds.; NATO ASI Series 15; Kluwer: Dordrecht, The Netherlands, 1995.

(3) (a) Miller, J. S. *Adv. Mater.* **2002**, *14*, 1105. (b) Gatteschi, D.; Sessoli, R. *Angew. Chem., Int. Ed.* **2003**, *42*, 268. (c) Miller, J.-S.; Epstein, A.-J. *Angew. Chem., Int. Ed. Engl.* **1994**, *33*, 385.

(4) (a) Ohba, M.; Okawa, H. *Coord. Chem. Rev.* **2000**, *198*, 313. (b) Batten, S. R.; Murray, K. S. *Coord. Chem. Rev.* **2003**, *246*, 103. (c) Lescouëzec, R.; Toma, L. M.; Vaissermann, J.; Verdaguer, M.; Delgado, F. S.; Ruiz-Pérez, C.; Lloret, F.; Julve, M. *Coord. Chem. Rev.* **2005**, *249*, 2691.

(5) (a) Ribas, J.; Escuer, A.; Monfort, M.; Vicente, R.; Cortés, R.; Lezama, L.; Rojo, T. *Coord. Chem. Rev.* **1999**, *193*, 1027. (b) Wang, X.-Y.; Wang, Z.-M.; Gao, S. *Chem. Commun.* **2008**, 281. (c) Escuer, A.; Aromí, G. *Eur. J. Inorg. Chem.* **2006**, 4721. (d) Zeng, Y.-F.; Hu, X.; Liu, F.-C.; Bu, X.-H. *Chem. Soc. Rev.* **2009**, *38*, 469.

(6) (a) Goher, M. A. S.; Mautner, F. A. *Croat. Chem. Acta* **1990**, *63*, 559. (b) Vicente, R.; Bitschnau, B.; Egger, A.; Sodin, B.; Mautner, F. A. *Dalton Trans.* **2009**, 5120. (c) Escuer, A.; Vicente, R.; Goher, M. A. S.; Mautner, F. A. *Inorg. Chem.* **1996**, *35*, 6386.

(7) (a) Mondal, K. C.; Mukherjee, P. S. *Inorg. Chem.* **2008**, *47*, 4215. (b) Gu, Z.-G.; Xu, Y.-F.; Yin, X.-J.; Zhou, X.-H.; Zuo, J.-L.; You, X.-Z. *Dalton Trans.* **2008**, 5593. (c) Yang, Y.-T.; Luo, F.; Che, Y.-X.; Zheng, J.-M. *J. Mol. Struct.* **2008**, *888*, 253. (d) Gu, Z.-G.; Zuo, J.-L.; You, X.-Z. *Dalton Trans.* **2007**, 4067.

(8) (a) Goher, M. A. S.; Cano, J.; Journaux, Y.; Abu-Youssef, M. A. M.; Mautner, F. A.; Escuer, A.; Vicente, R. *Chem.—Eur. J.* **2000**, *6*, 778. (b) Mautner, F. A.; Cortes, R.; Lezama, L.; Rojo, T. *Angew. Chem., Int. Ed. Engl.* **1996**, *35*, 78. (c) Mautner, F. A.; Hanna, S.; Cortes, R.; Lezama, L.; Barandika, M. G.; Rojo, T. *Inorg. Chem.* **1999**, *38*, 4647.

(9) (a) Liang, S. L.; Liu, Z. L.; Liu, C. M.; Di, X. W.; Zhang, J.; Zhang, D. Q. *Z. Anorg. Allg. Chem.* **2009**, *635*, 549. (b) Mautner, F. A.; Öhrström, L.; Sodin, B.; Vicente, R. *Inorg. Chem.* **2009**, *48*, 6280. (c) Fu, A. H.; Huang, X. Y.; Li, J.; Yuen, T.; Lin, C. L. *Chem.—Eur. J.* **2002**, *8*, 2293.

(10) (a) Liu, C.-M.; Yu, Z.; Xiong, R.-G.; Liu, K.; You, X.-Z. *Inorg. Chem. Commun.* **1999**, *2*, 31. (b) Shen, H.-Y.; Liao, D.-Z.; Jiang, Z.-H.; Yan, S.-P.; Sun, B.-W.; Wang, G.-L.; Yao, X.-K.; Wang, H.-G. *Chem. Lett.* **1998**, 469. (c) Escuer, A.; Vicente, R.; Mautner, F. A.; Goherc, M. A. S.; Abu-Youssef, M. A. M. *Chem. Commun.* **2002**, 64. (d) Yang, Q.; Zhao, J.-P.; Hu, B.-W.; Zhang, X.-F.; Bu, X.-H. *Inorg. Chem.* **2010**, *49*, 3746. (e) Liu, J.-C.; Fu, D.-G.; Zhuang, J.-Z.; Duan, C.-Y.; You, X.-Z. *J. Chem. Soc., Dalton Trans.* **1999**, 2337.

Published on Web 08/12/2010

Chart 1. 4,4′-Dipyridinio-*N*,*N*′-diacetate (top) and 4,4′-Dipyridinio-1-acetate (L, bottom)

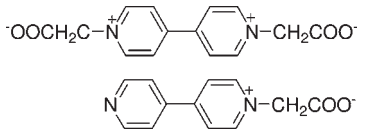

few anionic host networks with embedded cationic guests (Cs^+ or Me_4N^+).[8] A fruitful strategy toward 3D frameworks is to incorporate an organic bridging coligand into the metal-azide systems.[6b,9−12] Thus far, the most widely used second bridges are N-donors such as bis(pyridyl) and bis(azolyl) derivatives.[9,10a,b,11a,b,12a,b] The resulting 3D structures most often contain one-dimensional (1D) and two-dimensional (2D) azide-bridged motifs interlinked by organic bridges, offering good opportunities for inspecting the crossing area between low- and high-dimensional magnetic systems.[11,12] Less commonly, azide-bridged 3D networks are formed, in which the organic bridges are embedded and serve as additional supports reinforcing the 3D networks.[6b,9,10] Such compounds provide additional models for inspecting the systems with 3D magnetic exchange through short bridges. Overall, 3D metal-azide systems are still much limited compared with the large number of 1D and 2D systems. A literature survey indicates that only about 20 compounds with 3D azide-bridged networks, either with or without additional supporting bridges, have been structurally and magnetically investigated, the metal ions concerned being mainly Cu(II)[7,10e] and Mn(II),[6,8,10a−d] and in a few cases, Co(II)[9a,b] and Fe(II).[9c]

Pyridinecarboxylate derivatives such as isonicotinate and nicotinate have recently been used to construct magnetic coordination polymers with mixed azide and carboxylate bridges,[5d,10d,13] including a 3D Mn(II)-azide network with embedded organic bridges.[10d] To systematically investigate the construction and magnetism of the systems with simultaneous azide and carboxylate bridges, we have been exploring the approach using dipyridinium-based inner-salt-type dicarboxylate ligands (e.g., Chart 1, top).[14] It has been demonstrated that the zwitterionic ligands can lead to 1D, 2D, or 3D systems with interesting magnetic properties such as ferromagnetic coupling[14b,c] and solvent-modulated metamagnetism.[14a] In these systems, the negatively charged polynuclear clusters, chains, or layers with simultaneous azide and carboxylate bridges are interlinked by positively charged pyridinium spacers; however, no 3D azide and carboxylate bridged networks have been obtained. We now employ a bipyridine-derived monocarboxylate ligand, 4,4′-bipyridinio-1-acetate (L, Chart 1, bottom). Such zwitterionic ligands containing both pyridine and carboxylate coordinative groups remain unexplored in coordination chemistry. Here we report two different coordination polymers, $[Co_2(L)_2(N_3)_4(H_2O)]\cdot 4H_2O$ (**1**) and $[Mn_6(L)_4(N_3)_{12}(H_2O)]\cdot 5H_2O$ (**2**). Compound **1** consists of 1D coordination chains in which binuclear motifs with mixed (μ-EO-N_3)(μ-COO)$_2$ (EO = end-on) triple bridges are cross-linked by the 4,4′-dipyridinium-*N*-methylene spacers. This is the first Co(II) compound with these mixed bridges. Compound **2** exhibits a novel 3D Mn(II)-azide network with embedded organic ligands. Magnetic studies revealed that the mixed (μ-EO-N_3)(μ-COO)$_2$ triple bridges transmit ferromagnetic coupling in the Co(II) compound, and extended antiferromagnetic interactions exist in the Mn(II) compound.

Experimental Section

Physical Measurements. Elemental analyses were determined on an Elementar Vario ELIII analyzer. The FT-IR spectra were recorded in the range of 500−4000 cm^{-1} using KBr pellets on a Nicolet NEXUS 670 spectrophotometer. Temperature-dependent magnetic measurements were carried out on a Quantum Design SQUID MPMS-5 magnetometer with an applied field of 1 kOe, and diamagnetic corrections were made with Pascal's constants. The phase purity of the samples has been confirmed by powder X-ray diffraction, which was measured on a Bruker D8−Advance diffractometer equipped with Cu Kα at a scan speed of 1° min^{-1}.

Synthesis. The reagents were obtained from commercial sources and used without further purification. [HL]Br was prepared according to the literature.[15]

Caution! *Although not encountered in our experiments, azide compounds of metal ions are potentially explosive. The materials should be handled in small amounts and with care.*

$[Co_2(L)_2(N_3)_4(H_2O)]\cdot 4H_2O$ (1). A mixture of $CoCl_2\cdot 6H_2O$ (0.20 mmol, 0.048 g), [HL]Br (0.10 mmol, 0.030 g), and NaN_3 (1.6 mmol, 0.10 g) in 8 mL of water was stirred for 10 min at room temperature. Slow evaporation of the solution at room temperature yielded red crystals of **1** within 3 days. Yield: 50% based on Co. Anal. Found: C, 35.57; H, 3.95; N, 28.24%. Calcd for $Co_2C_{24}H_{30}N_{16}O_9$: C, 35.83; H, 3.76; N, 27.86%. Characteristic IR bands: $\nu_{as}(N_3)$, 2089 and 2045 cm^{-1}; $\nu_s(N_3)$, 1340 cm^{-1}; ν_{as}(COO), 1665 cm^{-1}; ν_s(COO), 1386 cm^{-1}.

$[Mn_6(L)_4(N_3)_{12}(H_2O)]\cdot 5H_2O$ (2). A mixture of $MnCl_2\cdot 4H_2O$ (0.20 mmol, 0.040 g), [HL]Br (0.10 mmol, 0.030 g), and NaN_3 (1.6 mmol, 0.10 g) in 4 mL of water was stirred for 10 min at room temperature. Slow evaporation of the solution at room temperature yielded yellow crystals of **2** within 1 week. Yield: 45% based on Mn. Anal. Found: C, 32.10; H, 3.35; N, 33.88%. Calcd for $Mn_6C_{48}H_{52}N_{44}O_{14}$: C, 32.05; H, 2.91; N, 34.26%. Characteristic IR bands: $\nu_{as}(N_3)$, 2107 and 2072 cm^{-1}; $\nu_s(N_3)$, 1350 cm^{-1}; ν_{as}(COO), 1645 cm^{-1}; ν_s(COO), 1393 cm^{-1}.

X-ray Crystallographic Measurements. Diffraction data for **1** and **2** were collected at 296 K on a Bruker Apex II CCD area detector equipped with graphite-monochromated Mo Kα radiation (λ = 0.71073 Å). Empirical absorption corrections were applied using the SADABS program.[16] The structures were

(11) (a) Fu, A.; Huang, X.-Y.; Li, J.; Yuen, T.; Lin, C. L. *Chem.—Eur. J.* **2002**, *8*, 2239. (b) Cheng, L.; Zhang, W.-X.; Ye, B.-H.; Lin, J.-B.; Chen, X.-M. *Eur. J. Inorg. Chem.* **2007**, 2668. (c) Chen, H.-J.; Mao, Z.-W.; Gao, S.; Chen, X.-M. *Chem. Commun.* **2001**, 2320.

(12) (a) Gao, E.-Q.; Wang, Z.-M.; Yan, C.-H. *Chem. Commun.* **2003**, 1748. (b) Gao, E.-Q.; Liu, P.-P.; Wang, Y.-Q.; Yue, Q.; Wang, Q.-L. *Chem.—Eur. J.* **2009**, *15*, 1217. (c) Gao, E.-Q.; Yue, Y.-F.; Bai, S.-Q.; He, Z.; Yan, C.-H. *J. Am. Chem. Soc.* **2004**, *126*, 1419.

(13) (a) Liu, F.-C.; Zeng, Y.-F.; Zhao, J.-P.; Hu, B.-W.; Sanudo, E.-C.; Ribas, J.; Bu, X.-H. *Inorg. Chem.* **2007**, *46*, 7698. (b) Liu, F.-C.; Zeng, Y.-F.; Li, J.-R.; Bu, X.-H.; Zhang, H.-J.; Ribas, J. *Inorg. Chem.* **2005**, *44*, 7298. (c) Zeng, Y.-F.; Liu, F.-C.; Zhao, J.-P.; Cai, S.; Bu, X.-H.; Ribas, J. *Chem. Commun.* **2006**, 2227. (d) Hu, B.-W.; Zhao, J.-P.; Sanudo, E.-C.; Liu, F.-C.; Zeng, Y.-F.; Bu, X.-H. *Dalton Trans.* **2008**, 5556. (e) Zeng, Y. F.; Zhao, J. P.; Hu, B. W.; Hu, X.; Liu, F. C.; Ribas, J.; Ribas-Arino, J.; Bu, X. H. *Chem.—Eur. J.* **2007**, *13*, 9924. (f) He, Z.; Wang, Z.-M.; Gao, S.; Yan, C.-H. *Inorg. Chem.* **2006**, *45*, 6694.

(14) (a) Sun, W.-W.; Tian, C.-Y.; Jing, X.-H.; Wang, Y.-Q.; Gao, E.-Q. *Chem. Commun.* **2009**, 4741. (b) Ma, Y.; Zhang, J.-Y.; Cheng, A.-L.; Sun, Q.; Gao, E.-Q.; Liu, C.-M. *Inorg. Chem.* **2009**, *48*, 6142. (c) Ma, Y.; Wen, Y.-Q.; Zhang, J.-Y.; Gao, E.-Q.; Liu, C.-M. *Dalton Trans.* **2010**, *39*, 1846. (d) Wang, Y.-Q.; Zhang, J.-Y.; Jia, Q.-X.; Gao, E.-Q.; Liu, C.-M. *Inorg. Chem.* **2009**, *48*, 789. (e) Tian, C.-Y.; Sun, W.-W.; Jia, Q.-X.; Tian, H.; Gao, E.-Q. *Dalton Trans.* **2009**, 6109. (f) Wang, Y.-Q.; Jia, Q.-X.; Wang, K.; Cheng, A.-L.; Gao, E.-Q. *Inorg. Chem.* **2010**, *49*, 1551.

(15) Surpateanu, G.; Depature, L.; Fourmentin-Lamotte, S. *Eur. Polym. J.* **1999**, *35*, 663.

solved by the direct method and refined by the full-matrix least-squares method on F^2, with all non-hydrogen atoms refined with anisotropic thermal parameters.[17] All the hydrogen atoms attached to carbon atoms were placed in calculated positions and refined using the riding model, and the hydrogen atoms of all water molecules in **1** and the coordinated water molecules in **2** were located from the difference maps. The hydrogen atoms of the lattice water molecules of **2** were not located. A summary of the crystallographic data, data collection, and refinement parameters for complexes **1** and **2** are provided in Table 1.

Results and Discussion

Crystal Structures. Compound 1. Single-crystal X-ray analysis revealed that compound **1** consists of 1D neutral polymeric chains in which binuclear $[Co_2(N_3)(COO)_2]_n$ subunits are interlinked by the L ligands. The relevant parameters are summarized in Table 2. As shown in Figure 1, there are two crystallographically independent Co(II) atoms. Co1 assumes a *mer*-octahedral $[N_3O_3]$ coordination geometry defined by three azide nitrogen atoms (N3, N11, and N14), two carboxylate oxygen atoms (O2 and O4A), and a water molecule (O5) (Figure 1). The Co1−N(O) distances range from 2.070(6) to 2.175(8) Å. Co2 is also octahedrally coordinated but in the *cis*-$[N_4O_2]$ environment composed of three azide nitrogens (N5, N8, and N14), a pyridine nitrogen, and two carboxylate oxygens (O1 and O3A). The Co2−N(O) bond distances fall in the range between 2.069(7) and 2.169(8) Å. A pair of Co1 and Co2 atoms are triply linked by an EO azide and two *syn-syn* carboxylates to give a binuclear $[Co_2(N_3)(COO)_2]_n$ subunit. To our knowledge, such a mixed bridging mode for Co(II) is unprecedented in the literature. The Co1···Co2 distance spanned by the $(\mu\text{-}N_3)(\mu\text{-}COO)_2$ triple bridge is 3.6 Å, and the Co1−N−Co2 angle is 115.1(4)°. For comparison, the Co···Co distances and Co−N−Co angles for the $(\mu\text{-}N_3)(\mu\text{-}COO)$ double bridges observed in a few previous Co(II) compounds are about 3.74−3.78 Å and 121.8−123.9°, respectively,[13f] suggesting that the addition of a carboxylate bridge reduces the distance and angle. These parameters for the $(\mu\text{-}N_3)(\mu\text{-}COO)_2$ triple bridge in **1** fall in the ranges for a few Mn(II) chains with similar triple bridges (Mn···Mn = 3.6−3.8 Å; Mn−N−Mn = 111−118°).[14e,f]

Neighboring $[Co(\mu\text{-}N_3)(\mu\text{-}COO)_2Co]$ binuclear motifs in **1** are linked by pairwise L ligands to an infinite zigzag-shaped chain, which contains 24-membered $[Co(L)_2Co]$ bimetallacycles with Co···Co = 11.25(8) Å (Figure 1). The L ligand in **1** serves as a μ_3,η^3 bridge spanning two binuclear units, with the carboxylate group in the *syn-syn* bridging mode. The two pyridyl rings in the ligand are relatively rotated by dihedral angles at about 29.2 and 4.6° for two crystallographic independent L ligands.

The parallel chains are packed down the *a* direction in a coplanar and corner-in-corner fashion and associated with each other through hydrogen bonds. Consequently, a sheet of coplanar zigzag chains is formed (Supporting Information, Figure S1). The sheets are further stacked into a 3D architecture through hydrogen bonds. The nearest interchain Co···Co distances are 7.34 Å.

Table 1. Crystal Data and Structure Refinements for Compounds **1** and **2**

	1	**2**
empirical formula	$Co_2C_{24}H_{30}N_{16}O_9$	$Mn_6C_{48}H_{52}N_{44}O_{14}$
fw	804.50	1798.98
cryst syst	triclinic	triclinic
space group	$P\bar{1}$	$P\bar{1}$
a (Å)	9.869(9)	10.979(2)
b (Å)	13.050(11)	15.309(3)
c (Å)	15.189(13)	21.552(4)
α (deg)	113.065	81.932
β (deg)	93.032(19)	88.500(6)
γ (deg)	109.773(13)	85.318(7)
V (Å^3)	1654(2)	3574.2(13)
Z	2	2
D (g m^{-3})	1.615	1.672
μ (mm^{-1})	1.078	1.120
F(000)	824	1820
reflections collected	8551	41560
unique reflections	5706	13854
GOF on F^2	0.952	1.026
R_{int}	0.0768	0.0469
R_1 [$I > 2\sigma(I)$]	0.0982	0.0600
wR_2 (all data)	0.2827	0.1695

Table 2. Selected Bond Lengths [Å] and Angles [deg] for Compound **1**[a]

Co1−O2	2.083(7)	Co1−O4A	2.070(6)
Co1−N11	2.113(9)	Co1−O5	2.114(7)
Co1−N14	2.111(8)	Co1−N3	2.175(8)
Co2−O1	2.069(7)	Co2−O3A	2.077(7)
Co2−N5	2.072(9)	Co2−N8	2.132(10)
Co2−N14	2.117(8)	Co2−N2B	2.169(8)
Co1−N14−Co2	115.1(4)		

[a] Symmetry transformations used to generate equivalent atoms: A, $-x,-y+1,-z+1$; B, $-x-1,-y-1,-z$.

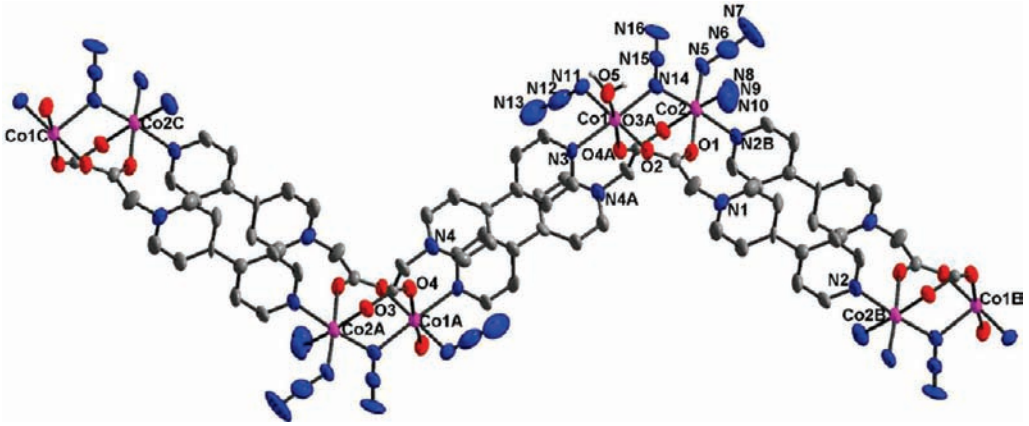

Figure 1. Local coordination environments of the Co(II) ions in compound **1**. Hydrogen atoms for C atoms are omitted for clarity and symmetry codes are A, $-x,-y+1,-z+1$; B, $-x-1,-y-1,-z$; C, $1+x,2+y,1+z$.

Table 3. Selected Distances [Å] and Angles [deg] for the Bridging Networks in **2**[a]

For [Mn1(μ-EO-N_3)$(COO)_2$Mn2] (motif B)			
Mn1−N1	2.153(4)	Mn1−O1	2.177(4)
Mn2−N1	2.212(4)	Mn2−O2	2.157(3)
Mn1−O4A	2.214(3)	Mn2−O3A	2.208(4)
Mn1−N1−Mn2	113.1(2)	Mn1···Mn2	3.641(8)
For [Mn3(μ-EO-N_3)$(COO)_2$Mn4] (motif C)			
Mn3−N4	2.172(4)	Mn3−O7	2.191(4)
Mn4−N4	2.209(4)	Mn4−O8	2.130(3)
Mn3−O6C	2.196(3)	Mn4−O5C	2.124(4)
Mn3−N4−Mn4	113.39(19)	Mn3···Mn4	3.662(9)
For Double EE-N_3			
Mn5−N13	2.271(5)	Mn5F−N15	2.164(6)
Mn5···Mn5F	5.371(11)		
Mn6−N31	2.280(6)	Mn6G-N33	2.241(6)
Mn6···Mn6G	5.439(14)		
For Single EE-N_3			
Mn5−N16	2.163(6)	Mn6−N18	2.191(6)
Mn5···Mn6	5.780(13)		
Mn2−N34	2.228(5)	Mn2···Mn2H	6.216(22)
Mn4−N36	2.243(5)	Mn4···Mn4i	6.046(21)
Mn2−N7	2.220(5)	Mn4−N9	2.249(4)
Mn2···Mn4	5.805(14)		
Mn5F−N30	2.219(6)	Mn6−N28	2.206(6)
Mn5F···Mn6	6.151(16)		
Mn5−N19	2.261(5)	Mn3D-N21	2.224(5)
Mn3D···Mn5	6.084(20)		
Mn6−N25	2.188(6)	Mn3D-N27	2.255(5)
Mn3D···Mn6	6.264(24)		
Mn1−N10	2.240(5)	Mn5−N12	2.219(5)
Mn1···Mn5	6.285(26)		

[a] Symmetry transformations used to generate equivalent atoms: A, $-x,-y+2,-z+1$; C, $-x,-y+1,-z+1$; D, $-x+2,-y+1,-z+1$; F, $-x+2,-y+1,-z+2$; G, $-x+2,-y,-z+2$; H, $-x+1,-y+2,-z+1$; I, $1-x,1-y,1-z$.

Compound 2. Single crystal X-ray analysis revealed that compound **2** crystallizes in a triclinic space group $P\bar{1}$ and consists of a 3D coordination framework. The relevant parameters are listed in Table 3. In the asymmetric unit of compound **2**, there are 6 crystallographic independent Mn(II) ions, 13 different azide ions (2 are located at inversion centers), 4 L ligands, 1 coordinated water molecule, and 5 guest water molecules (Figure 2). Mn1 assumes a disordered *mer*-octahedral [N_3O_3] coordination geometry defined by two azide nitrogen atoms (N1 and N10), two carboxylate oxygen atoms (O1 and O4A), a pyridine nitrogen atom (N45B), and a water molecule (O9). Differently, Mn2, Mn3, and Mn4 all adopt the *cis*-octahedral [N_4O_2] coordination geometry completed by two carboxylate oxygen atoms (O2 and O3A for Mn2; O7 and O6C for Mn3; O8 and O5C for Mn4), three azide nitrogen atoms (N1, N7, and N34 for Mn2; N4, N21D, and N27D for Mn3; N4, N9 and N36 for Mn4), and a pyridine nitrogen atom (N41 for Mn2; N39E for Mn3, and N43 for Mn4). Still differently, Mn5 and Mn6 are located in [N_6] octahedral environments with all donor atoms arising from azide ligands. The Mn−O/N distances around all Mn ions are in the narrow normal range of 2.124(4)−2.326(4) Å. Of the 13 independent azide ions, only one acts as terminal ligand (N22−N23−N24 to Mn6), two are in the EO bridging mode, and all the others adopt the EE bridging mode. The EO azide bridges appear simultaneously with carboxylate bridges in the *syn-syn* mode to form mixed (μ-EO-N_3)$(COO)_2$ triple bridges between Mn1 and Mn2 or between Mn3 and Mn4. The EE azides appears as single or double bridges between Mn(II) ions. Through these azide bridges, the neighboring Mn(II) ions are connected into a very complicated and unprecedented 3D Mn-azide network. The important parameters for these bridges are given in Table 3. It is evident that the Mn···Mn distances (d) for these bridges vary as follows: d[(EO-N_3)$(COO)_2$] (ca. 3.6 Å) ≪ d[(EE-N_3)$_2$] (ca. 5.4 Å) < d(EE-N_3) (ca. 5.8−6.3 Å). These parameters lie in the usual ranges for the different bridges.

To clearly elucidate the rather complicated 3D network formed through azide and carboxylate bridges, we resolve the network into three polynuclear motifs that can be defined as secondary building units (SBUs).[18] As shown in Figure 3, motif A is a centrosymmetric and rhombic tetranuclear cluster, in which alternating Mn5 and Mn6 are linked by single EE azide bridges and the two diagonal Mn5 ions are linked by double EE azides; motifs B and C are two independent dinuclear units with (EO-N_3)-$(COO)_2$ triple bridges, [Mn1(μ-EO-N_3)$(COO)_2$Mn2] (B) and [Mn3(μ-EO-N_3)$(COO)_2$Mn4] (C). These SBUs are linked into two different chains (I and II). Chain I is a homoleptic Mn(II)-azide chain formed by double EE azide bridges connecting the Mn6 ions from neighboring tetranuclear clusters (motif A). Chain II is a zigzag-shaped chain, in which motifs B and C alternating in the B−B−C−C sequence are connected by three independent single EE azide bridges: two centrosymmetric ones for B−B (or Mn2···Mn2H) and C−C (Mn4···Mn4I) connections, respectively, and an asymmetric one for B−C (Mn2···Mn4). Both chains I and II run along the b direction and are connected into a 3D network through further EE azide bridges (each chain I is connected to four chains II, and vice versa. Figure 3a). There are two different interchain connecting modes: along the [101] plane, Mn3 from chain II is connected to Mn5 and Mn6 from chain I through two azides, while along the [10−1], Mn1 from chain II to Mn5 from chain I through a single azide. Better understanding of the 3D connection can be facilitated by the topological analysis in terms of node- or vertex-based nets. In the above 3D azide-bridged network, motifs B and C can be reduced to 3-connected nodes, each connected to an A, a B, and a C motif, while motif A acts as 6-connected node, each connected to two A, two B, and two C motifs. Consequently, the 3D network is reduced to an unprecedented 3,6-connected binodal net with Schläfli symbol $(6.7^2)_4(6^2\cdot7^8\cdot8^2\cdot10^3)$ (Figure 3b). This peculiar net features the linear and zigzag chains that are aligned in parallel and connected in four directions.

The 3D azide-bridged network in **2** exhibits two different sets of 1D channels along the b direction, and the channel is occupied by the L ligands, which link the opposite dinuclear motifs across the channel (Figure 4, top). The L ligands in the smaller channel serve as bridges

(16) Sheldrick, G. M. *SADABS, Program for Empirical Absorption Correction of Area Detector Data*; University of Göttingen: Göttingen, Germany, 1996.

(17) Sheldrick, G. M. *SHELXTL*, version 5.1; Bruker Analytical X-ray Instruments Inc.: Madison, WI, 1998.

(18) Yaghi, O. M.; O′ Keeffe, M.; Ockwig, N. W.; Chae, H. K.; Eddaoudi, M.; Kim, J. *Nature* **2003**, *423*, 705.

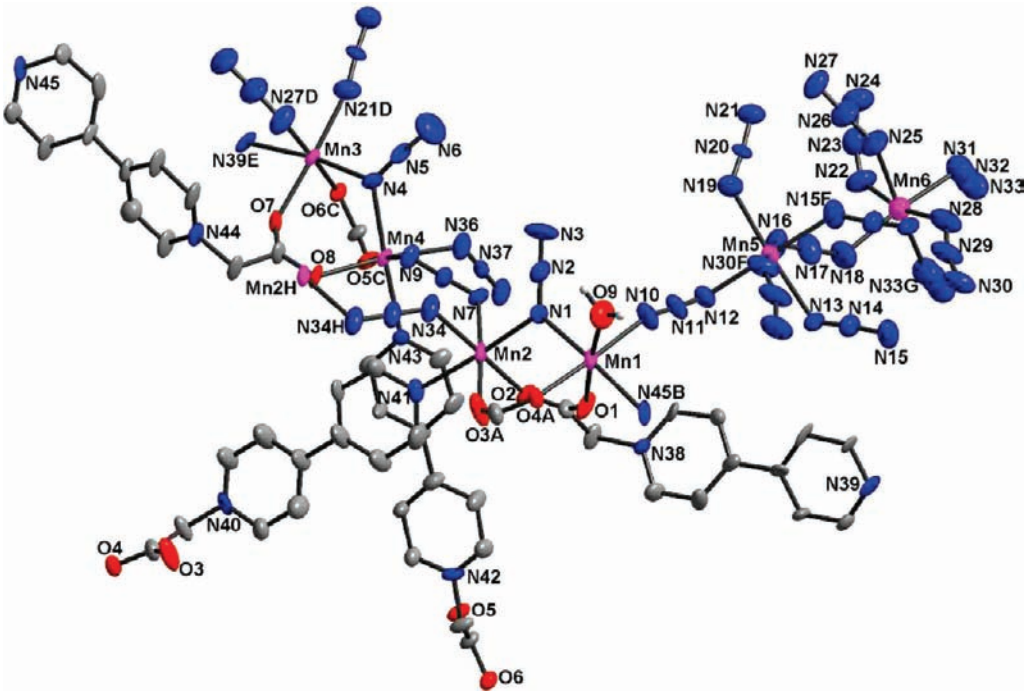

Figure 2. Local coordination environments of the Mn(II) ions in compound **2**. Hydrogen atoms for C atoms are omitted for clarity and symmetry codes are A, $-x,-y+2,-z+1$; B, $x,y,z+1$; C, $-x,-y+1,-z+1$; D, $-x+2,-y+1,-z+1$; E, $x,y,z-1$; F, $-x+2,-y+1,-z+2$; G, $-x+2,-y,-z+2$; H, $-x+1,-y+2,-z+1$.

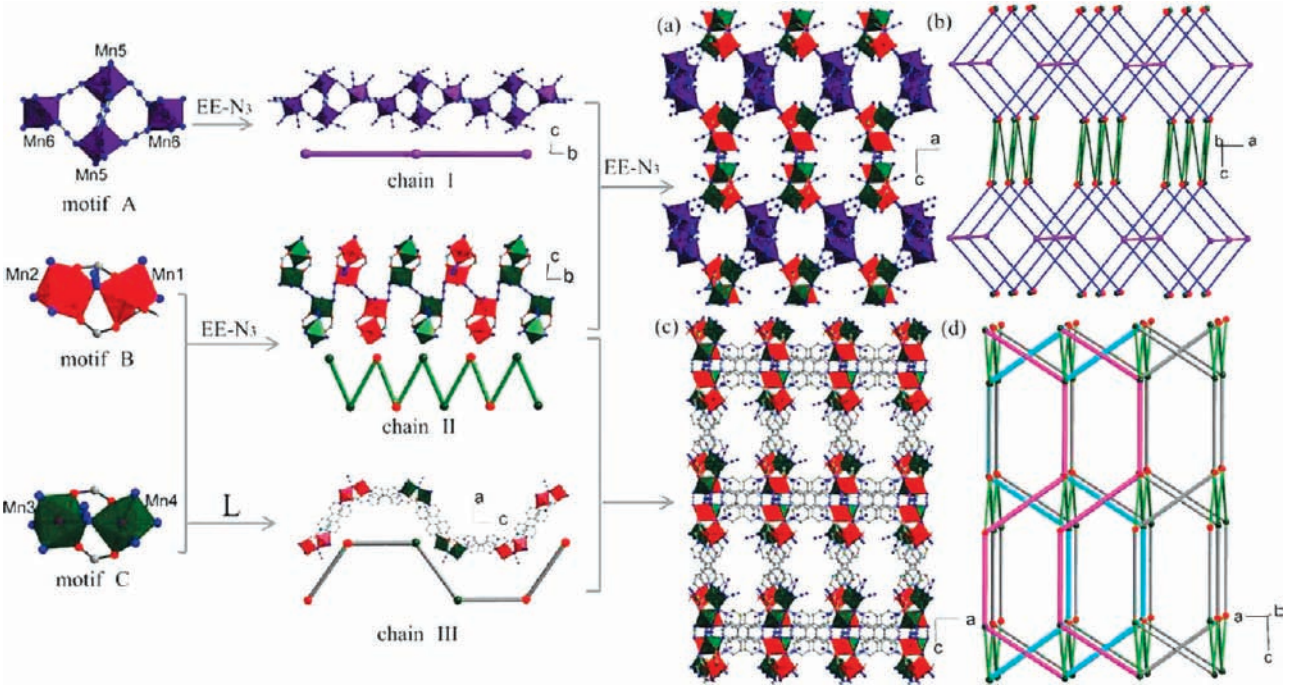

Figure 3. Different dimensional units in compound **2**: A, B, and C are the polynuclear motifs; I, II, and III represent the different 1D chains; (a) the 3D metal-azide framework; (b) the topology of the 3D metal-azide framework; (c) the 3D framework without the A motifs; (d) the topology of the 3D framework without the A motifs.

between motifs B and C, while those in the larger channels are between two motifs B or between two motifs C. Taking into account the L spacers, motifs B and C are both 5-connected nodes, and the whole 3D Mn-azide-L network represents an unprecedented 5,5,6-connected trinodal $(3\cdot6^8\cdot7)_4(3^2\cdot6^2\cdot7^{10}\cdot10)$ net (Figure 4, bottom), which is derived by connecting the 3-connected nodes in the former 3,6-connected net.

An alternative description of the structure is to consider the characteristic chain motif formed from the L ligands. As shown in Figure 3, motifs B and C alternating in the B−B−C−C sequence are connected by pairwise L ligands to formed an infinite $[MnL]_n$ chain (chain III, Figure 3) along the crystallographic (01−2) direction. This doubly bridged chain is similar to that in compound **1**, but with a sinusoidal, instead of zigzag, conformation. The difference

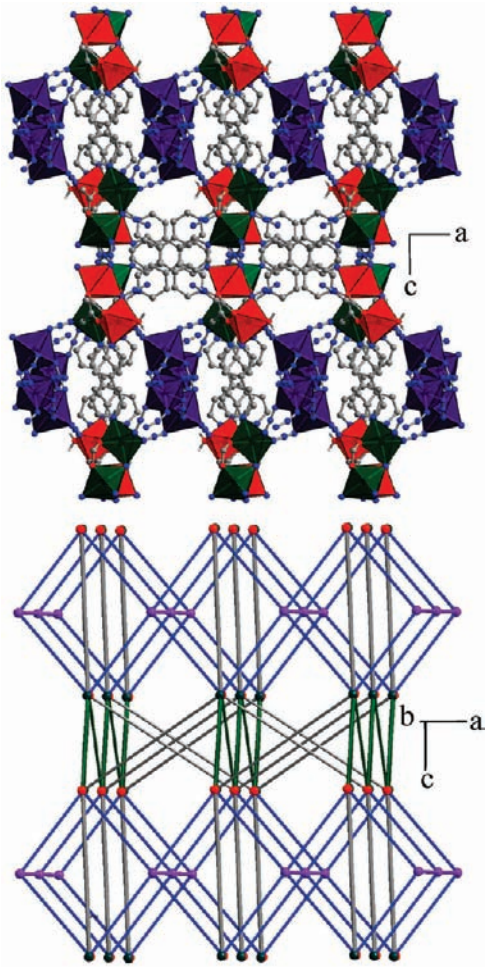

Figure 4. 3D architecture (top) and topology (bottom) of compound **2**.

is mainly due to the flexibility of the ligand arising from the methylene group. The L-bridged chains (type III) and the azide-bridged zigzag chains (type II) along different directions share the binuclear SBUs (motifs B and C) to give a 3D network (Figure 3c), which can be reduced to a diamond network, with both B and C motifs as 4-connected nodes (Figure 3d). This 3D subnetwork contains 1D channels along the *b* direction, which are occupied by the homoleptic Mn(II)-azide chains (type I) along the same direction. The whole 3D network is formed by chain I being connected to the channel walls via EE-azide bridges.

Magnetic Properties. Compound 1. The magnetic susceptibility (χ) of compound **1** was measured on a crystalline sample under 1 kOe in the range of 2−300 K (Figure 5). The χT value per formula at 300 K is about 6.48 cm^3 K mol^{-1}, much larger than the spin-only value (3.75 cm^3 K mol^{-1}) for two $S = 3/2$ spins, but falling in the expected range for high-spin octahedral Co(II) with significant contribution from unquenched orbital momentum. Upon cooling, while the χ value shows monotonic increase, the χT value increases smoothly to a rounded maximum at 65 K, and then decreases rapidly down to 3.57 cm^3 K mol^{-1} at 2 K (Figure 5). The data above 65 K follow the Curie−Weiss law with $C = 6.37$ cm^3 K mol^{-1} and $\theta = 7.81$ K. The positive θ value indicates the domination of the ferromagnetic coupling in the high temperature range.

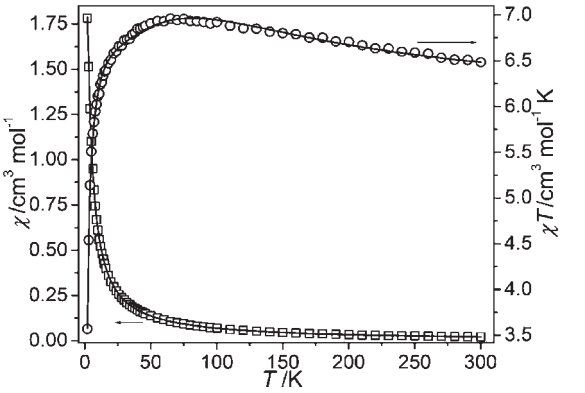

Figure 5. Temperature dependence of χ and χT for **1** under 1 kOe. The solid lines represent the best fit to the appropriate model (see text).

The decrease of χT values below 65 K is mainly due to spin−orbital coupling of Co(II).

According to the structural data, the system can magnetically be treated as a binuclear compound in which magnetic coupling is mediated through the triple bridge (μ-N_3)(μ-$COO)_2$. To evaluate the interactions, we used the empirical approach proposed recently by Lloret et al. based on spin Hamiltonian[19]

$$\hat{H} = -(25/9)\hat{S}^{A}_{eff}\cdot\hat{S}^{B}_{eff} - G(T,J)\beta H(\hat{S}^{A}_{eff} + \hat{S}^{B}_{eff})$$

The magnetic susceptibility of the dicobalt systems can be expressed as[20]

$$\chi_{dinuclear} = \frac{2N\beta^2[G(T,J)]^2}{kT}\frac{1}{3+\exp[(25/9)J/(kT)]} \quad \text{(Eq1)}$$

Where the Co(II) ions are assumed to have an effective spin of $S_{eff} = 1/2$, and $G(T, J)$ is a fictitious Landé factor dependent upon λ (spin−orbital coupling parameter), α (orbital reduction factor), Δ (axial distortion factor of the octahedral field), and J (intradimer magnetic exchange). The molecular field approximation was applied to account for any interdimer interactions:[1b]

$$\chi = \frac{\chi_{binuclear}}{1 - zj'(N\beta^2)^{-1}[G(T,J)]^{-2}\chi_{binuclear}} \quad \text{(Eq2)}$$

where zj' is the parameter that describes the interactions between binuclear motifs. The experimental data can be fit well by the above equations, the best-fit parameters being $J = 10.3$ cm^{-1}, $\alpha = 1.44$, $\Delta = 389$ cm^{-1}, $\lambda = -70$ cm^{-1}, and $zj' = 0.98$ cm^{-1}. The α and Δ values fall in the usual ranges expected for six-coordinated Co(II) complexes, and the λ value is slightly lower than usual values (90−180 cm^{-1}).[19] Considering the approximation of the model, these parameters should be taken as a rough estimation. Nevertheless, the positive J value confirms the ferromagnetic interactions through the mixed (μ-EO-N_3)-(μ-$COO)_2$ bridges. No magnetic information on such triple bridges between Co(II) ions is available in the literature, but ferromagnetic interactions have been reported

(19) Lloret, F.; Julve, M.; Cano, J.; Ruiz-García, R.; Pardo, E. *Inorg. Chim. Acta* **2008**, *361*, 3432.
(20) Lines, M. E. *J. Chem. Phys.* **1971**, *55*, 2977.

for Co(II) chain compounds with triple (μ-EO-N_3)$_2$(μ-COO)[14b,c,21] and double (μ-EO-N_3)(μ-COO)[13f] bridges. By contrast, the three types of mixed bridges all propagate antiferromagnetic interactions in Mn(II) compounds. The dependence of the nature of magnetic interactions upon metal ions has also been recognized for some other bridges such as dicyanoamide[4b,22] and *syn-anti* carboxylate,[14b,23] and this can be attributed to the different electronic configurations [$t_{2g}^5e_g^2$ for Co(II) and $t_{2g}^3e_g^2$ for Mn(II)] of the metal ions:[14b,23] the unpaired electrons in e_g orbitals favor ferromagnetic interactions, whereas those in t_{2g} orbitals favor antiferromagnetic interactions. The small positive zJ' value suggests that weak ferromagnetic interactions may be operative between the binuclear units.

Compound 2. The magnetic susceptibility of compound **2** was measured on a crystalline sample under 1 kOe in the range of 2−300 K (Figure 6). The χT value per Mn(II) for compound **2** at 300 K is about 3.39 cm^3 K mol^{-1}, lower than the value expected for an isolated Mn(II) ion (4.375 cm^3 K mol^{-1}). As the temperature is lowered, the χT value decreases monotonically, while the χ value increases to an approximate plateau between 22 and 15 K, and then increases upon further cooling. The data above 36 K follow the Curie−Weiss law with C = 4.26 cm^3 K mol^{-1} and θ = −72.31 K. The above features indicate overall antiferromagnetic coupling between the Mn(II) centers. The antiferromagnetism is also supported by the isothermal magnetization measured at 2 K. The magnetization increases slowly and linearly with increased field, and the value of 0.43 Nβ at 50 kOe is much lower than the expected saturation value of 5 Nβ (Supporting Information, Figure S3).

According to the structural data, there are up to 13 different magnetic exchange pathways in the 3D network of **2**, including two independent (COO)$_2$(EO-N_3) triple bridges, two independent (EE-N_3)$_2$ double bridges, and nine independent EE-N_3 single bridges. It is impossible to quantitatively evaluate the magnetic exchange parameters in such a complicated system. However, it has been well established that EE azide bridges, whether double or single, always mediate antiferromagnetic coupling, with $|J|$ in the range 2−16 cm^{-1}.[5a,24−26] The mixed (COO)$_2$(EO-N_3) triple bridges have been found in a few Mn(II) chain compounds, and they also mediate antiferromagnetic coupling interactions in the order of several cm^{-1}, whether the bridges are double or triple.[11c,13f,14b−f] Therefore, we could safely assume that all the bridging motifs in **2** mediate antiferromagnetic coupling, and the compound is a 3D antiferromagnet. Typical 3D antiferromagnets should show maxima in $\chi-T$ plots at certain temperatures. The maximum of **2** appears at about 22 K. The observed plateau below 22 K and the subsequent rise in χ can be due to the presence of any paramagnetic impurity: the decrease in χ for the 3D network is compensated and then overcompensated by the increase in χ for the paramagnetic impurity.

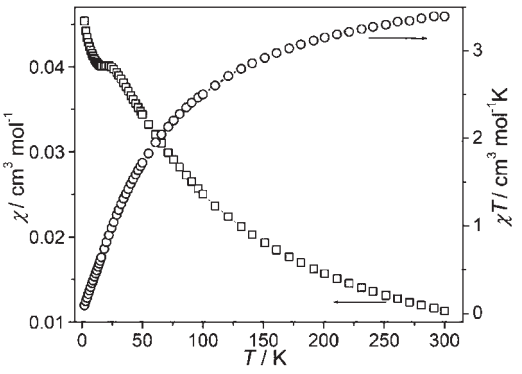

Figure 6. Temperature dependence of χ and χT for **2** under 1 kOe (the solid lines are only the guide of eye).

Conclusions

We have described two transition metal coordination polymers with azide and zwitterionic ligands bearing both carboxylate and pyridine groups. Compound **1** consists of 1D coordination chains built of dinuclear motifs with mixed (μ-EO-N_3)(μ-COO)$_2$ triple bridges, while **2** exhibits a complicated 3D Mn(II)-azide network with unprecedented topology, the zwitterionic ligands serving as embedded supports for the 3D structure. Magnetic studies revealed that the mixed (μ-EO-N_3)(μ-COO)$_2$ triple bridges transmit ferromagnetic coupling between Co(II) ions. Compound **2** shows 3D antiferromagnetism, with the azide-only and the simultaneous azide-carboxylate bridges all inducing antiferromagnetic interactions between Mn(II) ions. This study reveals that the bipyridine-based zwitterionic monocarboxylate ligand can lead to novel magnetic systems different from those derived from the dicarboxylate analogues. Extended studies along this line are underway in this laboratory.

Acknowledgment. The authors thank NSFC (20771038), and Shanghai Leading Academic Discipline Project (B409) for financial support.

Supporting Information Available: Crystallographic data in CIF format, and supplementary structural graphics are available. This material is available free of charge via the Internet at http://pubs.acs.org.

(21) Liu, T.; Zhang, Y.-J.; Wang, Z.-M.; Gao, S. *Inorg. Chem.* **2006**, *45*, 2782.

(22) (a) Batten, S. R.; Jensen, P.; Kepert, C. J.; Kurmoo, M.; Moubaraki, B.; Murray, K. S.; Price, D. J. *J. Chem. Soc., Dalton Trans.* **1999**, 2987. (b) Kmety, C. R.; Huang, Q.; Lynn, J. W.; Erwin, R. W.; Manson, J. L.; McCall, S.; Crow, J. E.; Stevenson, K. L.; Miller, J. S.; Epstein, A. J. *Phys. Rev.* **2000**, *B 62*, 5576. (c) Nuttall, C. J.; Takenobu, T.; Iwasa, Y.; Kurmoo, M. *Mol. Cryst. Liq. Cryst.* **2000**, *342*, 227. (d) Goodenough, J. B. *Magnetism and the Chemical Bond*; Wiley: New York, 1963.

(23) Coronado, E.; Galán-Mascarás, J. R.; Gómez-García, C. J.; Murcia-Martínez, A. *Chem.—Eur. J.* **2006**, *12*, 3484.

(24) Gao, E.-Q.; Bai, S.-Q.; Yue, Y.-F.; Wang, Z.-M.; Yan, C.-H. *Inorg. Chem.* **2003**, *42*, 3642, and references therein.

(25) (a) Goher, M. A. S.; Abu-Youssef, M. A. M.; Mautner, F. A.; Vicente, R.; Escuer, A. *Eur. J. Inorg. Chem.* **2000**, 1819. (b) Escuer, A.; Vicente, J. R.; Goher, M. A. S.; Mautner, F. A. *Inorg. Chem.* **1995**, *34*, 5707. (c) Ju, Z.-F.; Yao, Q.-X.; Wu, W.; Zhang, J. *Dalton Trans.* **2008**, 355. (d) Bitschnau, B.; Egger, A.; Escuer, A.; Mautner, F. A.; Sodin, B.; Vicente, R. *Inorg. Chem.* **2006**, *45*, 868.

(26) (a) Wang, X.-Y.; Wang, L.; Wang, Z.-M.; Su, G.; Gao, S. *Chem. Mater.* **2005**, *17*, 6369. (b) Abu-Youssef, M. A. M.; Escuer, A.; Langer, V. *Eur. J. Inorg. Chem.* **2005**, 4659. (c) Gao, E.-Q.; Cheng, A.-L.; Xu, Y.-X.; He, M.-Y.; Yan, C.-H. *Inorg. Chem.* **2005**, *44*, 8822. (d) Ma, Y.; Cheng, A.-L.; Sun, W.-W.; Zhang, J.-Y.; Gao, E.-Q. *Inorg. Chem. Commun.* **2009**, *12*, 412. (e) Escuer, A.; Vicente, R.; Goher, M. A. S.; Mautner, F. A. *J. Chem. Soc., Dalton Trans.* **1997**, 4431.